



Reduction of CO₂ Emissions and Durability Assessment of Concrete Incorporating Recycled Aggregates, Steel Fibers, and Polycarboxylate Ether Nano-superplasticizers

M. Saravanan^{1*} and R. Nirmala²

¹Department of Civil Engineering, P.B. College of Engineering, Irungattukottai, Chennai, TN, India

²Department of Civil Engineering, Satyabhama Institute of Science and Technology, Chennai, TN, India

Received: 11.01.2025 Accepted: 09.03.2025 Published: 30.03.2025

*saravanan.sathyabamacivil@gmail.com



ABSTRACT

Natural aggregates used in concrete are expensive, and their mining process is inherently disruptive to the environment. Additionally, the enormous volume of construction waste generated strains the ecosystems considerably. One promising alternative is addressing the challenges of concrete production and achieving environmental sustainability by producing recycled aggregates from leftover concrete. While Recycled Fine Aggregate (RFA) is rarely utilized in structural concrete, Recycled Coarse Aggregate (RCA) is increasingly recognized in structural applications and regulations. This research aims to replace the conventional fine and coarse particles in concrete with both RCA and RFA. To further enhance the performance of recycled aggregate concrete and promote sustainability, Polycarboxylate Ether (PCE) nano-superplasticizers were incorporated into the mix; they improve workability, reduce the water-cement ratio, and enhance particle dispersion, leading to improved strength and durability in concrete. The study specifically investigates the impacts of using 100% recycled coarse aggregate, 10% recycled fine aggregate, and steel fibers in place of natural aggregates. The results show increased slump value when recycled concrete aggregate (100% RCA and 10% RFA) replaces natural aggregate. Additionally, the combination of recycled materials (100% RCA with 10% RFA) and the addition of 2% steel fibers demonstrated superior durability properties compared to conventional concrete. This substitution not only enhances durability but also offers a more sustainable alternative to traditional construction practices.

Keywords: CO₂ Emissions; Steel Fibers; Polycarboxylate Ether (PCE) Nano-superplasticizers; Recycled Aggregate Concrete (RAC); Recycled Coarse Aggregate (RCA); Durability properties.

1. INTRODUCTION

The realm of construction extensively embraces concrete, a remarkable composite forged from cement, aggregates, and water. However, with the waves of economic growth and the evolution of infrastructure, a tidal wave of construction waste inevitably surges forth. The management of demolition and construction refuse constitutes a hefty share of solid waste, with a substantial portion finding its final resting place in landfills. Embracing Recycled Aggregate (RA) stands as a pivotal stride toward sustainable evolution in the concrete sector and the stewardship of construction waste. RA serves as a promising substitute for natural aggregate, playing a crucial role in environmental conservation (Kisku *et al.* 2017). Nonetheless, Recycled Aggregate Concrete (RAC) faces certain hurdles in the realm of practical engineering (Ashish and Saini, 2018). Primarily, the diverse origins and treatment methods of reused aggregates render their mechanical properties somewhat unpredictable. Bao *et al.* (2020) revealed that RAC tends to display inferior mechanical and durability

characteristics compared to Natural Aggregate Concrete (NAC). In addition, the recycled aggregate's heightened water absorption rate coupled with the diminished durability of the resulting concrete imposes limitations on its use in structures necessitating longevity and resilience. Furthermore, meticulous sieving is crucial to procure high-quality recycled aggregate, which escalates the production expenses of RAC (Liao *et al.* 2024). Therefore, investigating and addressing the mechanical and durability attributes of recycled aggregate emerges as vital to amplify their practical worth, encourage the adoption of recycled aggregate, and mitigate environmental impacts. Guo *et al.* 2018; Kannan *et al.* 2021 elucidated that the mechanical and durability properties of concrete containing Recycled Coarse Aggregate (RCA) were typically inferior in comparison to those devoid of RCA. This shortcoming is attributed to the sub-par quality of RCAs stemming from the porous character of the adhered mortar, which leads to diminished mechanical strength and durability-related properties (Wardeh *et al.* 2015). Bui *et al.* (2017) discovered that an increase in the replacement rate of

RCA correlates with a decline in the mechanical properties of RAC. Similarly, Verma and Ashish, (2017) indicated that a high replacement rate of RCA results in a decrease in compressive strength. Evidence suggests that substituting natural coarse aggregate with RCA at a replacement level of 25-50% exerts minimal impact on the workability and mechanical properties of concrete (Kou and Poon, 2009; Limbachiya *et al.* 2012; Rao *et al.* 2011). Beyond a 50% replacement threshold, the mechanical characteristics of concrete utilizing RCA are significantly inferior compared to those crafted with natural aggregate (Poon *et al.* 2002; Xiao *et al.* 2012). Consequently, the use of RCA at elevated replacement levels is confined to non-structural applications within the construction sector. RCA is increasingly being embraced in guidelines for structural applications, while the employment of Recycled Fine Aggregate (RFA) in structural concrete remains constrained. It is widely recognized that the infusion of steel fibers enhances the mechanical attributes of concrete by bolstering ductility, crack resistance, and toughness (Amirtharaj and Vinod, 2018; Gholampour and Ozbakkaloglu, 2018; Karatas *et al.* 2019; Ibrahim *et al.* 2021).

Steel fibers also mitigate the overall ecological impact of construction by enhancing the longevity of structures crafted with steel fiber-reinforced concrete (Senaratne *et al.* 2016; Ramkumar and Kannan, 2022). Research is scarce on the characteristics of fiber-reinforced concrete incorporating RCA. Carneiro *et al.* 2014; Guo *et al.* 2014 revealed that the infusion of steel fibers boosts the fracture toughness of concrete composed with RCA. Gao and Zhang, 2018 discovered that the presence of steel fibers significantly enhances the flexural strength of concrete containing RCA. Erdem *et al.* 2011 indicated that the inclusion of steel fibers can curtail the natural development of microcracks in RCA-infused concrete through meticulous micro-structural analysis. Afroughsabet *et al.* 2017 uncovered that incorporating steel fibers diminishes water retention and drying shrinkage in concrete comprising RCA. They observed that concrete formulated with 100% RCA and 1% steel fiber exhibited merely a slight increase in water absorption compared to the unreinforced natural aggregate concrete. The majority of current studies have highlighted the potential of steel fibers in augmenting the qualities of concrete formulated with RCA. Nevertheless, most of these investigations focused primarily on assessing the mechanical and durability properties of concrete made solely with RCA. Research examining the durability properties of concrete fashioned from both RCA and RFA is notably limited. Therefore, this study attempts to explore the durability properties of concrete created with both RCA and RFA as substitutes for natural coarse and fine aggregate. This exploration is crucial as it holds the promise of extending the lifespan of concrete structures while potentially fostering more environmentally responsible construction practices by minimizing waste and reliance on virgin materials.

Concrete production significantly contributes to global CO₂ emissions, primarily due to cement manufacturing, but Polycarboxylate Ether (PCE) nano-superplasticizers play a pivotal role in reducing its carbon footprint. By enhancing cement hydration efficiency, they enable the production of high-strength concrete with reduced cement content, directly lowering CO₂ emissions. These superplasticizers also improve the performance of concrete containing recycled aggregates, such as RCA and RFA, promoting the use of sustainable alternatives to natural aggregates while conserving resources and minimizing the environmental impact of mining. Additionally, their ability to enhance flow properties reduces the energy required for mixing, placement, and compaction, contributing to energy savings during construction. The increased durability of concrete with PCE nano-superplasticizers reduces the need for frequent repairs or replacements, extending its service life and further conserving resources. Furthermore, their compatibility with supplementary cementitious materials (SCMs) such as fly ash and slag allows for the substitution of high-carbon-footprint Portland cement with eco-friendly alternatives. In summary, PCE nano-superplasticizers not only enhance concrete performance but also drive sustainability by reducing CO₂ emissions, conserving resources, and supporting environment-friendly construction practices.

Table 1. Chemical composition of Cement

Component	Cement (%)
Silicon dioxide (SiO ₂)	21.92
Aluminium oxide (Al ₂ O ₃)	5.42
Iron oxide (Fe ₂ O ₃)	4.94
Magnesium oxide (MgO)	1.41
Calcium oxide (CaO)	59.84
Na ₂ O	0.29
K ₂ O	0.67

Table 2. Properties of Steel fibers

Properties	Hooked-end
Density (kg/m ³)	7850
Tensile strength (MPa)	1650
Elastic modulus (N/mm ²)	2.1 x 10 ⁵
Specific gravity	7.5
Length (mm)	40
Diameter (mm)	0.60
Aspect ratio (AR)	70

2. MATERIALS

2.1 Materials

To assess the bond strength, sample blocks were made using materials such as cement, fly ash, fine and

coarse aggregate, superplasticizer, and bar. All the samples concrete had normal strength. The grade 53 Ordinary Portland Cement (OPC) that complied with IS 12269 was utilized. Initial setting time, ultimate setting time, fineness, consistency, and specific gravity were found to be 3.15, 309 m²/kg, 31%, 45 minutes, and 450 minutes, respectively. Table 1 displays the cement's chemical makeup. As a fine aggregate, M-sand, which is classified as Zone-II in the IS-383 specification, was employed. M-sand's specific gravity and fineness modulus were found to be 2.6 and 2.7, respectively. Well-graded angular granite that agreed with IS: 383-1970 and had a maximum size of 12.5 mm was used as the coarse material. The coarse aggregate's specific gravity, fineness modulus, and water absorption rate were 2.7, 7.2, and 0.62%, respectively. Potable water was added to the concrete. A polycarboxylate ether-based super-plasticizer was used to make concrete mixes with low water-to-binder ratios workable; this super-plasticizer complies with ASTM C 494-13.

2.1.1 M-sand

This study uses M-sand conforming to Zone-II as per the specifications of IS383 as Fine Aggregate (FA). The specific gravity and fineness modulus of M-sand were 2.62 and 2.71.

2.1.2 Coarse Aggregates

Well-graded angular granite stone that complied with IS: 383-1970 with a maximum size of 12.5 mm was utilized as coarse aggregate. The coarse aggregate's specific gravity, fineness modulus, and water absorption were 2.70, 7.20, and 0.62%, respectively.

2.1.3 Polycarboxylate Ether (PCE) Nano-superplasticizers

The water-reducing admixture, Polycarboxylate Ether nano-superplasticizers, with a high specific gravity of 1.82 and 25% solid content, was employed as a critical additive in concrete to enhance its performance. These PCE nano-superplasticizers significantly reduced the water-cement ratio without compromising workability, leading to the production of high-strength and durable concrete. By improving the dispersion of cement particles, they enhance hydration efficiency and contribute to a denser microstructure. Additionally, their advanced formulation allows for better compatibility with SCMs and recycled aggregates, enabling the creation of more sustainable and environment-friendly concrete mixes. The high solid content ensures optimal performance at lower dosages, making them an efficient solution for achieving desired concrete properties while promoting eco-friendly construction practices.

2.1.4 Steel Fibers

Steel fibers with hooked ends that complied with ASTM A820-01 were employed in this analysis.

Steel fibers with a volume fraction of between 0.5% - 2% were used in this analysis. The length, diameter, and aspect ratio of the fibers are presented in Table 2.

3. EXPERIMENTATIONS

3.1 Mix Proportioning

The mix portioning for M25 grade concrete was made as per IS: 10262-2019 guidelines to achieve the target strength of the concrete (Sampathkumar *et al.* 2024). After various trials, an optimized mix was arrived which gives the target strength as presented in Table 3. With those optimized mix ratios, the concrete mix was made to test its workability and mechanical properties. Initially, the fine aggregate and the recycled coarse aggregate were given as input into the mixer for 120 s. Then, the needed quantity of cement was added to the mixture and mixed for the same duration without adding water content to the mixture. This process is followed by the inclusion of steel fiber in the mixture. Finally, the superplasticizer mix along with the water was added to the mixer and mixed for 240 s.

Table 3. Mix Proportioning of M25 Grade RAC (kg/m³)

Properties	M1 (Control mix)	M2 (100% RCA 10% RFA)	M3 (100% RCA 10% RFA+0.5% SF)	M4 (100% RCA 10% RFA+1% SF)	M5 (100% RCA 10% RFA + 1.5% SF)	M6 (100% RCA 10% RFA+2% SF)
Cement (kg/m ³)	342.10	342.10	342.10	342.10	342.10	342.10
Water (kg/m ³)	143.68	143.68	143.68	143.68	143.68	143.68
Natural Fine Aggregate (kg/m ³)	699.31	629.41	629.41	629.41	629.41	629.41
Natural Coarse Aggregate (kg/m ³)	1223.89	-	-	-	-	-
Recycled Fine Aggregate (kg/m ³)	-	69.9	69.9	69.9	69.9	69.9

3.2 Tests

3.2.1 Water Absorption Test

As per the ASTM C-642, the water absorption rate of natural aggregate concrete and recycled aggregate concrete cube samples were measured. The cured test samples were dried and the density was determined by the mass and volume using the division process. The

cured test samples were heated at 100 °C for 24 hours and their weight and volume were measured (W_d). Simultaneously, a few samples were submerged in water; after 24 hours, the samples were wiped dry, and the wet mass of the samples was measured (W_s). The water absorption rate of the natural and recycled aggregate concrete cube samples was measured using Eqn. (1):

$$\text{Water absorption (\%)} = [(W_s - W_d) / (W_d)] \times 100 \dots (1)$$

where, W_d = dry weight of specimen (kg) and W_s = saturated weight of specimen (kg).

3.2.2 Rapid Chloride Penetration Test (RCPT)

Abiding by the standard ASTM C1202, the ability of natural and recycled aggregate concrete to resist the penetration of chloride ions was measured by employing the Rapid Chloride Penetration Test (RCPT). The concrete test specimens of 50 mm thickness and 100 mm diameter were employed for this analysis as depicted in Fig. 1. The test specimen was allowed to curing for 28 days. After the 28 days of curing, the concrete samples were vacuum saturated. After the saturation of samples, the concrete samples were sealed with a non-conductive coating. Then, the specimen was placed between the two cells of the RCPT test apparatus, where one cell was filled with Sodium chloride (NaCl) solution and another cell was filled with Sodium hydroxide (NaOH) solution. A 60 V DC was applied to the cells for 6 hours. The assessment of the RCPT rating is based on the coulombs of charge transmitted vs. the penetration of chloride ions, as outlined in Table 4.



Fig. 1: RCPT Test Bench

Table 4. RCPT ratings as per ASTM C1202

Charge passed (Coulombs)	Chloride ion penetrability
>4500	High
2000–4500	Moderate
500–2000	Low
100–500	Very Low
<100	Extremely Low (negligible)

3.2.3 Sorptivity Test

Abiding by the standard ASTM 1585, a test sample in the sorptivity test absorbs water through capillary action. Consequently, the capillary action-induced rate of water absorption was expanded as a water sorptivity metric. The sorptivity of the concrete specimen was determined using Eqn. (2):

$$I = St^{1/2} \dots (2)$$

where, S is the sorptivity, t is the time taken, and I is the capillary ingress of water (in mm).

3.2.4 Chemicals Attack Tests

According to ASTM-C289 (2007), this test was aimed to determine the decline in compressive potential while subjected to alkaline, acidic, and sulfate solutions. Meanwhile, ASTM-C1152/C1152M (2020) was utilized for the strength reduction evaluation in response to the acid solution. Concrete cubes were cured for 28, 56, and 90 days. At each interval, 12 cubes were exposed to different conditions: immersion in water containing 3% NaOH, 3% MgSO₄, and 3% H₂SO₄ solutions. After the curing periods (28, 56, and 90 days), the cubes from the solutions were removed, and their compressive strengths were measured.

3.2.5 Water Permeability Test

According to IS 3085 (1965), the specimen concrete that was properly cured and tested for 28 days was employed. The specimen was saturated under a vacuum to ensure that no air pockets were present in the specimen. Then, the concrete specimens were placed in the testing cell of the permeability apparatus. Proper sealing of the specimen in the cell was ensured to prevent leakage of water around the sample. Connect the cell to a water reservoir and a pressure system. A constant water pressure was applied to the sample for a specified duration as per IS 3085 (1965). The pressure level normally ranges depending on the particular necessities of the test and the properties of the concrete. The quantity of water permeating through the sample over the testing period was measured. This can be done by collecting and estimating the water that has passed through the specimen. The total volume of water passed, the testing duration, and the applied pressure were recorded. The permeability coefficient based on the collected data and the dimension of the specimen was determined using the Eqn. (3):

$$K = \frac{Q}{AT\frac{H}{L}} \dots (3)$$

where, K is permeability coefficient (cm/s); Q is the water quantity; A is the area of the specimen face; T is

the time; $\frac{H}{L}$ is the ratio of the pressure head to the thickness of the specimen.

3.2.6 Micro-structural Analysis

The natural and recycled aggregate concrete was examined using X-ray Diffraction (XRD), Energy Dispersive Spectroscopy (EDS), and Scanning Electron Microscopy (SEM). The microscopic analysis was carried out using SEM, XRD, and EDAX on samples collected from 150 mm cube specimens tested for compressive durability for 28 days as shown in Fig. 2. The specimens were tested to estimate the morphology of the sample. On analyzing the distribution of concrete-to-pore, the structure of the matrix can be determined and contrasted with the control mix to estimate the thickness (Elanthikkalet *et al.* 2016). The X-ray analysis system was employed to incarcerate the SEM images (Fig. 2 & 3). The technique gives details of physical properties, crystallographic structure, and chemical composition. The data was deliberated at two theta (2θ) angles in the range of (0 to 100°) in intervals of 10° (Ganga and Senthil, 2023). The mineralogical composition (whether amorphous or crystalline) of the concrete mixes was analyzed using XRD, which is a widely utilized technique offering insights into both qualitative and quantitative phase analysis, providing specifics about distinct components. Through powder diffraction analysis, details about the structure, allotropic transformations, phase transitions, and purity were obtained. The samples were finely ground for XRD analysis, creating flat specimens on glass substrates with each sample affixed using an adhesive material. These specimens were then positioned in the designated slot and the diffracted intensities (peaks) were recorded using a powder diffractometer equipped with monochromatic copper K radiation.

Table 5. Results of RAC cubes immersed in HCl

Mix ID	M1	M2	M3	M4	M5	M6
Weight loss (%)	5	6	5.8	5.5	5.3	5
Strength loss (%)	10	12	11	10	9	8



Fig. 2: Samples collected and prepared for SEM testing



Fig. 3: SEM instrument

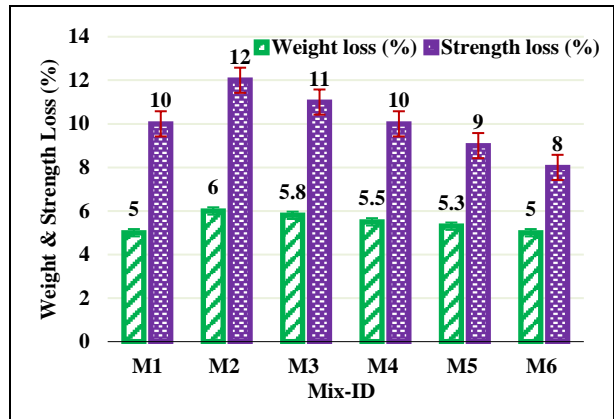


Fig. 4: Variation of strength and weight loss of various mixes against acid attack

4. RESULTS AND DISCUSSION

4.1 Acid Resistance of RAC

Table 5 shows the weight loss (%) of CC and RAC immersed in HCl solution. The results demonstrate the impact of recycled aggregate and steel fiber addition on concrete durability under acid attack.

At 28 days, M1 (Control mix) showed a 5% weight loss, and the M2 mix containing 100% RCA with 10% RFA showed a slightly higher weight reduction of 6%, demonstrating that the incorporation of recycled aggregate can increase vulnerability to acid attack. As steel fibers (SF) were added to the concrete mix (M3 to M6), a gradual reduction in weight loss was noticed. The M3 with 0.5% SF results in 5.8% weight loss, M4 with 1% SF presents 5.5% weight loss, M5 with 1.5% SF presents 5.3% weight loss, and M6 with 2% SF presents 5% weight loss, which almost matches with the weight loss value of M1 (Control mix). This trend demonstrates that increasing the steel fiber content improves the chemical resistance of the concrete. These outcomes justify that while recycled aggregates marginally

compromise concrete’s resistance to acid attack, the strategic addition of steel fibers can effectively counteract this degradation. The varying concentrations of SF in M3 to M6 give a clear indication of its beneficial role in improving the durability of concrete, particularly in aggressive environments. The strength loss (%) of the CC and RAC immersed in the HCl solution is also presented in Table 5. The control mix (M1) shows a strength loss of 10% at 28 days, showing the base level of durability against acidic conditions. Mix M2, which contains 100% RCA with 10% RFA shows a higher strength loss of 12% at 28 days as compared to the control mix (Fig. 4).

This implies that the incorporation of recycled aggregate materials can unfavourably influence the concrete resistance from acid attack, possibly because of inherent weaknesses like increased porosity and weaker interfaces within the recycled material. As steel fibers (SF) are introduced in the concrete mix from 0.5% to 2%, there is an observable improvement in strength retention. The strength for various mixtures is 11, 9, and 8%. The addition of steel fibers probably offers additional internal support in the concrete matrix, mitigating the structural damage caused by the acidic environment. Steel fibers can bridge cracks and enhance both the durability and mechanical properties, as upheld by earlier studies that recommend that steel fibers improve crack resistance and structural integrity under different stress conditions (Soroushian and Lee, 1990). Thus, these outcomes highlight the potential of using steel fibers in recycled aggregate concrete to improve its performance in a corrosive environment.

4.2 Alkaline Resistance of RAC

Table 6 shows the weight loss (%) of the CC and RAC immersed in NaCl solution. The test results present a discernible pattern of weight loss over time, featuring the impacts of different compositions on salt opposition.

Table 6. Results of RAC cubes immersed in NaCl

Mix ID	M1	M2	M3	M4	M5	M6	M6
Weight loss (%)	2	2.5	2.3	2.1	2	1.8	5
Strength loss (%)	5	6	5.5	5.2	5	4.8	8

At 28 days, the control mix (M1) shows a weight reduction of 2%. M2 mix, which contains 100 % RCA with 10% RFA shows a marginally higher weight loss of 2.5%, suggesting that the presence of RCA may mitigate weakness to salt infiltration to some extent, possibly because of their innately higher porosity and absorption properties as compared with natural aggregate concrete. As the steel fibers were added to the concrete mix, a gradual decrease in weight loss was observed for the M3-M6 mix. The weight loss of the M3-M6 mix was 2.3, 2.1, 2.5, and 1.8%. This indicates that steel fibers contribute positively towards improving the concrete’s

resistance to salt attack. The SF improves the structural cohesion within the concrete, decreasing the pathways for salt ingress and thus mitigating the material degradation over time; they can improve the crack resistance and tensile strength of the concrete, thus making it more resilient to external aggressive environment conditions (Brandt *et al.* 2009). These findings reveal that RA could marginally decrease the salt resistance of concrete by enhancing the durability of concrete.

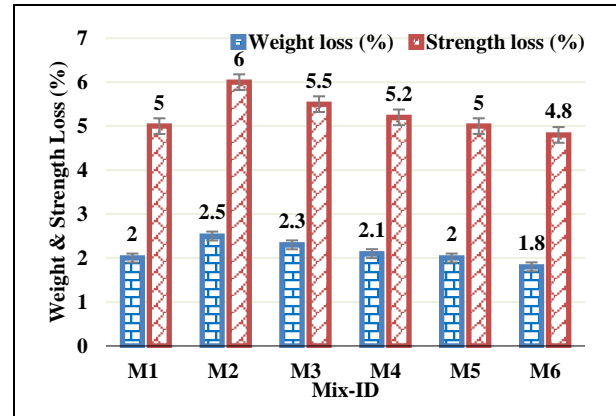


Fig. 5: Variation of strength and weight losses of various mixes against alkaline attack

Table 6 presents the strength loss (%) of the CC and RAC immersed in NaCl solution. The M1 (control mix) possesses a strength loss of 5% at 28 days. The M2 mix contains 100% RCA with 10% RFA and experiences the highest weight loss of 6% at 28 days, implying that the mix with higher RA might have increased vulnerability to chemical degradation processes like those induced by salt, potentially because of the higher porosity of recycled aggregates contrasted with natural aggregates. However, the addition of steel fibers (SF) into the concrete mix possesses gradual improvement in salt resistance *i.e.*, the weight loss was reduced as observed for the M3-M6 mix. The weight loss values of the M3-M6 mix were 5.5, 5.2, 5, and 4.8% as shown Fig. 5. This trend highlights the role of steel fibers in improving the structural integrity and durability of concrete. Steel strands are known to bridge microcracks that form within the concrete matrix, thus restricting the pathways for salt infiltration and decreasing the overall material degradation (ACI Panel 544, 1982). The outcomes show that while the utilization of recycled aggregates can increase the vulnerability of concrete to salt-induced degradation, the addition of steel fibers effectively mitigates this issue, thus improving the durability and longevity of the concrete under saline conditions.

4.3 Sulfate Resistance of RAC

Table 7 shows the strength loss (%) of the CC and RAC immersed in MgSO₄ solution. The results show

changing levels of weight loss across various concrete mixes, which represents the impacts of various material compositions on sulfate resistance.

Table 7. Results of RAC cubes immersed in MgSO₄

Mix ID	M1	M2	M3	M4	M5	M6
Weight loss (%)	1	1.5	1.4	1.2	1.1	1
Strength loss (%)	10	12	11	10.5	10	9.5

The M1 (control mix) shows a weight loss rate of 1% at 28 days. M2 mix with 100% RCA with 10% RFA exhibits an increased weight loss rate of 1.5% at 28 days. This higher rate of degradation compared to M1 demonstrates that recycled aggregate might have less resistance to sulphate exposure, possibly because of the existing cement paste in RCA, which might contribute to more prominent porosity and subsequently higher susceptibility to chemical attack. The inclusion of steel strands (SF) shows a progressive reduction in weight loss, demonstrating enhanced resistance to sulphate attack as observed for the M3-M6 mix. The weight loss value of the M3-M6 mix was 1.4, 1.2, 1.1, and 1%. The inclusion of steel fibers appears to enhance the concrete’s durability by improving its structural integrity and diminishing the permeability to sulphate ions. Steel fibers can bridge cracks within the concrete matrix, effectively restricting the ingress of destructive chemical ions and slowing the rate of degradation. These outcomes show that while the utilization of recycled aggregate could initially decrease the concrete resistance to sulphate attack, the addition of steel fibers can substantially lessen these adverse effects.

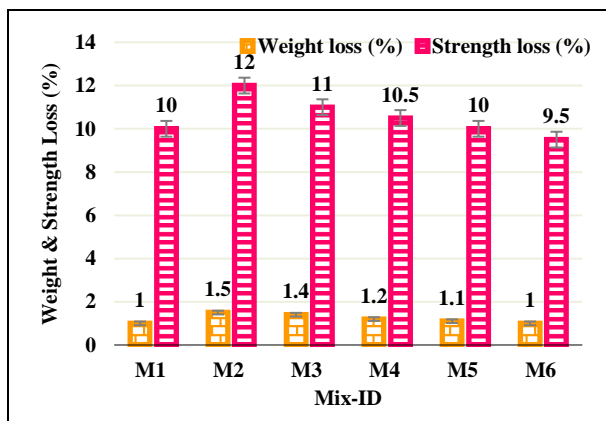


Fig. 6: Variation of strength and weight losses of various mixes against sulphate attack

The strength loss results of RAC cubes immersed in a MgSO₄ (Magnesium Sulfate) solution over 28 days are presented in Table 7. The M1 (control mix) shows a weight loss rate of 10% at 28 days. M2 mix exhibits an increased weight loss rate of 12% at 28 days. This can be attributed to the intrinsic properties of recycled aggregates, which frequently incorporate

remnants of old cement paste that increment the material’s porosity and susceptibility to chemical reactions like those happening in a sulfate-rich environment. The addition of SF into the concrete mix seems to lessen the adverse effect of recycled aggregate on concrete’s sulfate resistance observed for the M3-M6 mix. The strength loss values of the M3-M6 mix were 11, 10.5, 10, and 9.5%, as shown Fig. 6. The beneficial effect of steel fibers in concrete mixes such as M3, M4, M5, and M6 probably emerges from their capacity to improve the mechanical integrity of the concrete. Steel fibers work by bridging the microcracks and maintaining cohesion within the concrete matrix, which not only improves tensile strength but also reduces the permeability to harmful ions like sulphates.

4.4 Water Absorption of RAC

The water absorption test results for RAC show varying levels of absorption across various mixes, highlighting the impact of recycled aggregate and steel fiber on the porosity of concrete (Fig. 7).

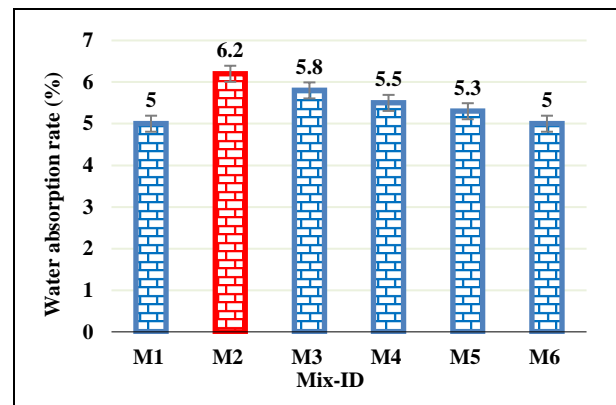


Fig. 7: Variation of water absorption rate of various mixes

The M1 (control mix) shows a water absorption rate of 5% at 28 days. M2 mix shows a water absorption rate of 6.2% for 28 days. The increased absorption rate can be ascribed to the advanced porosity of RA, which typically contains remnants of old cement paste that contribute to their increased capacity to absorb water. With the addition of steel fibers, a progressive reduction in water absorption rate was observed for the M3-M6 mix. The water absorption rates of the M3-M6 mix were 5.8, 5.5, 5.3, and 5%. The addition of steel fibers probably contributes to this reduced water absorption by improving the internal cohesion and structure of the concrete matrix. Steel fibers are known to enhance crack resistance and structural connectivity within the concrete, successfully diminishing the porosity and subsequently, the material’s susceptibility to water ingress. These outcomes delineate that the incorporation of steel fibers in recycled aggregate concrete can significantly reduce the adverse impact of increased porosity related to recycled aggregate materials.

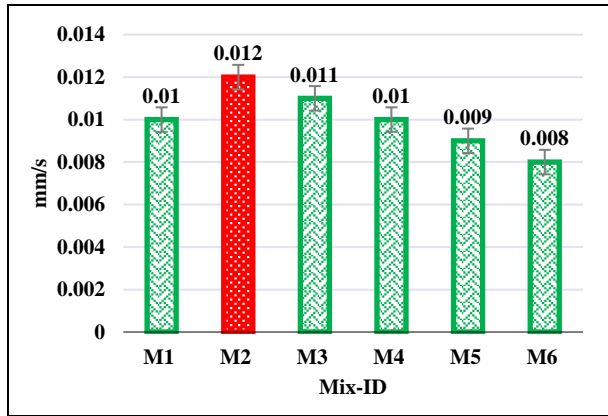


Fig. 8: Variation of Water Permeability of various mixes

4.5 Water Permeability of RAC

The water permeability test results for different RAC mixes are presented in Fig. 8. The M1 mix shows a reliable low penetrability value of 0.01 mm at 28 days. M2 mix, which includes 100% RCA with 10% RFA shows a water absorption rate of 0.012 mm/s at 28 days. This enhancement is attributed to the inherent properties of the recycled mixture, which often have a higher

porosity owing to the presence of aged cement paste, leading to increased water channels within the concrete matrix. The outcome of this study was found to be aligned with existing studies. Cheng *et al.* 2022 reported that the addition of RA prompted to increase in porosity. As the steel fiber was added to the concrete mix, a progressive reduction in the water permeability rate was observed for the M3-M6 mix. The water permeability rate of M3 was 0.011 mm/s, 0.010 mm/s with M4, 0.009 mm/s with M5, and 0.008 mm/s with M6, at 28 days.

The steel fibers probably contribute to this decreased permeability by bridging micro-cracks and improving the internal structure of the concrete, thus decreasing the pathways for water flow and improving overall durability. Notably, the addition of 2% of steel fibers (M6 mix) resulted in a more prominent decrease in the water permeability, which is almost 20% less than the M1 mix.

4.6 Chloride Penetration of RAC

The results of the Rapid Chloride Penetration Test (RCPT) for natural (M1) and recycled aggregate concrete (M2) mix were presented in Table. 8.

Table 8. RCPT test results of RAC in coulombs

Mix ID	M1 (Control mix)	M2 (100% RCA +10% RFA)	M3 (100% RCA + 10% RFA +0.5% SF)	M4 (100% RCA+10% RFA+1% SF)	M5 (100% RCA +10% RFA +1.5% SF)	M6 (100% RCA + 10% RFA + 2% SF)
28 days	2000	2500	2400	2200	2100	2000
56 days	1800	2300	2200	2000	1900	1800

Results from Rapid Chloride Permeability Test (RCPT) demonstrate significant differences in chloride ion penetration resistance between Conventional Concrete (CC) cured for 28 days and RAC tested at 56 days, with these variations primarily attributed to their distinct compositional properties. The M1 (control mix) displays a moderate chloride ion penetrability with values ranging from 1800 to 2000 coulombs at both 28 and 56 days, falling within the category of moderate penetrability as per ASTM C1202. On the other hand, the M2 mix containing 100% RCA with 10% RFA shows higher chloride penetration levels, demonstrating a possibly higher risk of chloride ingress (Bao *et al.* 2020). As steel fibers are added into the mix, there is a perceptible improvement in chloride particle penetrability, with values going from 1800 to 2400 coulombs at 28 days and 1800 to 2200 coulombs at 56 days, showing a shift towards the low to moderate penetrability range as per ASTM standards. The incorporation of steel fibers probably increases the resistance of concrete to the penetration of chloride ions by improving its overall durability and reducing the pathways for chloride ingress through crack bridging and densification of the concrete matrix. These outcomes

highlight the significance of considering both the synthesis of recycled aggregate and steel fibers to mitigate chloride ion penetrability and enhance the strength of concrete structures, particularly in chloride-rich environments such as marine or deicing salt-exposed structures (Yi *et al.* 2020).

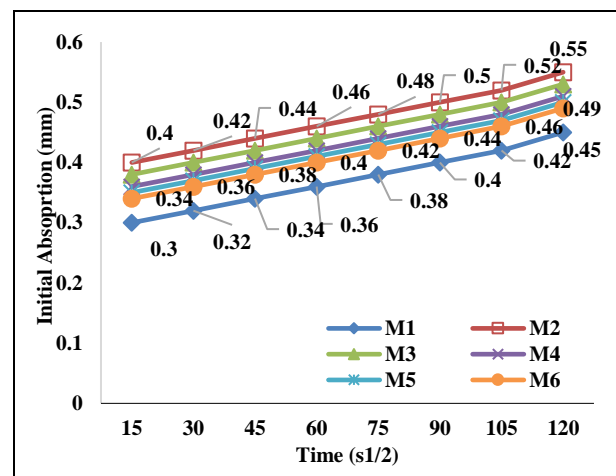


Fig. 9: Variation of Sorptivity of various mixes

4.7 Sorptivity Values of RAC

The ratio of the square root of the time is used to determine the quantity of sorption per unit area. The slope of the line of the optimum fit curve at the first stage (five minutes had passed) was known as initial sorptivity. Sorptivity test results of various concrete mixes reveal insightful trends regarding the water absorption characteristics of the concrete over time as depicted in Fig. 9 and Table 9.

The M1 (control mix) displays the most minimal sorptivity values with 0.30 mm at 15 s and increases to 0.45 mm at 120 s. M2 mix, which contains 100% RCA and 10% RFA shows the highest sorptivity values of 0.40 mm at 15 s and 0.55 mm at 120 s.

Table 9. Sorptivity results of RAC

Time (s ^{1/2})	M1	M2	M3	M4	M5	M6
15	0.30	0.40	0.38	0.36	0.35	0.34
30	0.32	0.42	0.40	0.38	0.37	0.36
45	0.34	0.44	0.42	0.40	0.39	0.38
60	0.36	0.46	0.44	0.42	0.41	0.40
75	0.38	0.48	0.46	0.44	0.43	0.42
90	0.40	0.50	0.48	0.46	0.45	0.44
105	0.42	0.52	0.50	0.48	0.47	0.46
120	0.45	0.55	0.53	0.51	0.50	0.49

The increased sorptivity in M2 can be ascribed to the intrinsically higher porosity of RA, which commonly has attached mortar remnants that increase their water absorption capacity, making RAC more susceptible to moisture ingress, potentially affecting durability. As SF was added to the concrete mix, a notable reduction in sorptivity was observed. The sorptivity values of M3, M4, M5, and M6 were 0.38, 0.36, 0.35, and 0.34 mm, for 15 s; these values were increased to 0.53, 0.511, 0.50 and 0.49 mm. Addition of steel fibers can decrease the sorptivity of the concrete by enhancing the micro-structure network and decreasing the quantity of open pores for water penetration. SF bridges the micro-cracks and improves cohesion within the concrete, effectively limiting the pathways through which water can be absorbed.

4.8 Microstructural Characterization of RAC

From the other durability test results, the M6 was found to offer better durability properties. Hence, the compressive tested samples of M6 mixes were used for micro-structural analysis and compared with M1 and M2 mixes. Fig. 12 depicts the SEM image of M6, which describes the micro-structural analysis of the M3-M6 concrete mix. The porous spaces and cavities were not highly found in the M3-M6 concrete, which indicates that the presence of fibers effectively bridges the crack and

thus avoids the formation of porous structures (Nanthini *et al.* 2024).

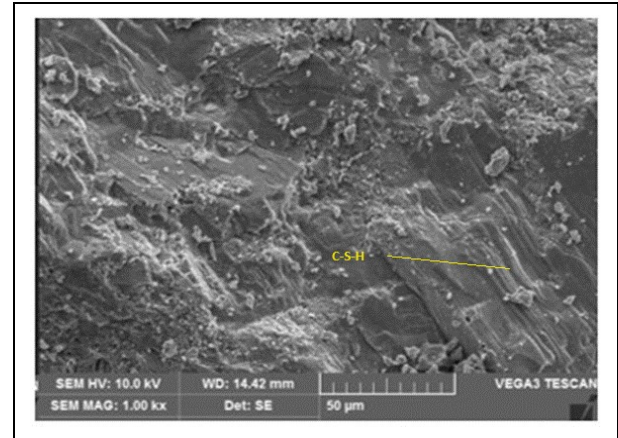


Fig. 10: SEM image of M1 samples

In the SEM image of CC, there were bright, angular particles that could be sand grains as shown in Fig. 10. In the SEM image of M2, a large number of porous spaces and cavities were found (Fig. 11), which indicates that the concrete is not properly compacted. In addition, more distinct and weaker ITZ was observed between the cement paste and aggregates.

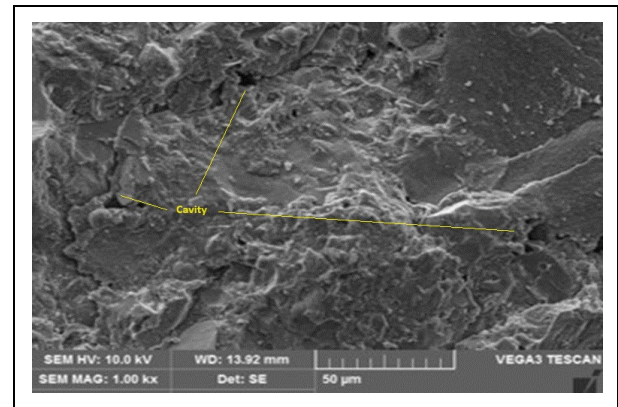


Fig. 11: SEM image of M2 samples

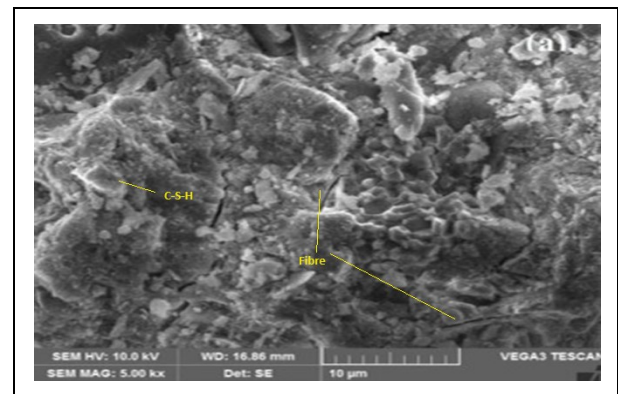


Fig. 12: SEM image of M6 samples

The EDX scheme of M1 depicts the major hike of Silica (Si) at 1.7 keV followed by oxygen (O) at 0.5 keV and Aluminum (Al) at 1.8 keV, as shown in Fig. 13. Most pronounced is the presence of silica (Si), which has a major peak at 1.7 keV, as expected since silica is a primary constituent of the aggregates (typically sand and gravel) used in concrete. Furthermore, silica reacts with calcium hydroxide during the hydration process of cement to form calcium silicate hydrate (C-S-H), the primary compound responsible for the strength and durability of concrete. Following silica, Oxygen (O) shows a significant peak at 0.5 keV. The presence of oxygen is attributed to its role in the formation of various oxides that constitute the aggregates and cement. These include silicon dioxide (SiO₂) and calcium oxide (CaO), which are fundamental to the cement's chemistry. Oxygen is crucial as it is part of the water (H₂O) needed for the hydration process and the resulting oxides and hydrates formed in hardened cement. Aluminum (Al) is also detected, with a notable peak at 1.8 keV. Although typically less abundant than silicon and oxygen, aluminum is an essential component of the cement's aluminosilicate phases. In Portland cement, small amounts of aluminum react with silica and calcium under hydration conditions to form calcium aluminate silicates, which are vital for the development of early strength and the regulation of setting time (Scrivener and Kirkpatrick, 2008).

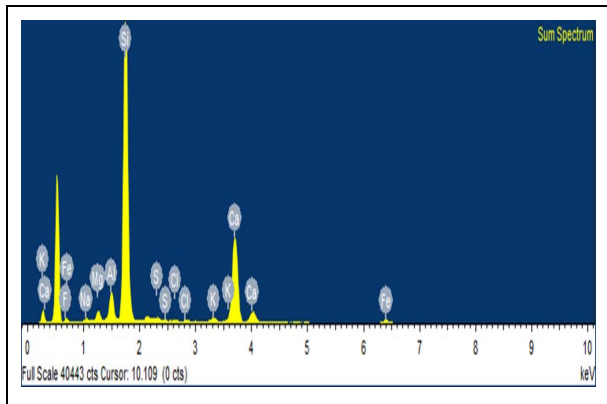


Fig. 13: EDX plot of M1 mix

The EDX plot of M6 samples shows the major peaks of Ca at 3.4 keV, followed by Si at 1.7 keV, O₂ at 0.5 keV, and Al at 1.5 keV (Fig. 14). The peak at 3.4 keV for Ca indicates its high presence. This aligns with the general understanding that calcium compounds play a vital role in the development of calcium silicate hydrates, which are indispensable for the progress of concrete durability. Similarly, the peak for Si at 1.7 keV underscores its substantial presence, primarily due to the silicon dioxide content in the aggregates and the Portland cement. Silicon dioxide reacts with calcium oxide under hydration to form additional calcium silicate hydrates, further contributing to the concrete's mechanical properties. The Oxygen (O) peak at 0.5 keV is also

prominent, which is predictable considering oxygen's role in forming oxides such as CaO and SiO₂ that make up the bulk of concrete materials. The presence of oxygen is pivotal for the chemical reactions during the cement hydration process. Additionally, the peak for Aluminum (Al) at 1.5 keV indicates the presence of aluminum compounds, which can be attributed to its minor component in the cement or as an impurity in the aggregates. Aluminum may participate in the formation of calcium aluminate hydrates, which also contribute to the setting and hardening process of concrete (Scrivener and Kirkpatrick, 2008).

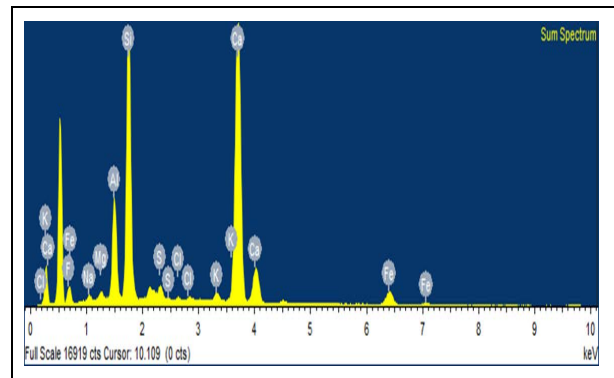


Fig. 14: EDX plot of M6 mix

5. CONCLUSION

The durability of Recycled Aggregate Concrete under acid attack is highlighted by the results from immersing RAC cubes in the HCl solution. The inclusion of RCA and RFA in the concrete mix drastically reduced its resistance to acid, alkali, sulphate, and chloride attacks; however, the addition of steel fibers helps regain the loss in resistance caused by the inclusion of RCA and RFA. It was found that as the quantity of steel fibers increased, the concrete's resistance to acid, alkali, sulphate, and chloride attacks improved significantly. Specifically, when 2% steel fibers were added (in the M6 mix), the concrete's resistance to these aggressive chemicals was notably enhanced. Moreover, steel fibers also help reduce water absorption and permeability in RAC by bridging cracks that inhibit the ingress of water. This trend highlights the effectiveness of steel fibers in enhancing the concrete's chemical resistance, likely due to their ability to reduce porosity and bridge cracks, thus improving the overall durability of the concrete in aggressive environments. In addition, the incorporation of PCE nano-superplasticizers in the mix further contributes to reducing the water-cement ratio and improving workability, resulting in a denser concrete structure with enhanced chemical resistance. The use of PCE nano-superplasticizers helps optimize the hydration process, improving the long-term durability and sustainability of the concrete while contributing to a reduction in CO₂ emissions by decreasing the need for

excessive cement content. These results affirm the dual benefits of incorporating recycled materials for sustainability while maintaining durability through the strategic use of steel fibers and the environmental advantages provided by the inclusion of PCE nano-superplasticizers.

FUNDING

This research received no specific grant from any funding agency in the public, commercial, or not-for-profit sectors.

CONFLICTS OF INTEREST

The authors declare that there is no conflict of interest.

COPYRIGHT

This article is an open-access article distributed under the terms and conditions of the Creative Commons Attribution (CC BY) license (<http://creativecommons.org/licenses/by/4.0/>).



REFERENCES

- Afroughsabet, V., Biolzi, L. and Ozbakkaloglu, T., Influence of double hooked-end steel fibers and slag on mechanical and durability properties of high performance recycled aggregate concrete, *Compos. Struct.*, 181, 273–284(2017). <https://doi.org/10.1016/j.compstruct.2017.08.086>
- Amirtharaj, J. and Vinod, K. R., Effect of fly ash on fiber reinforced concrete—A durability approach, *Int. Res. J. Eng. Technol.*, 5(12), 643–647 (2018).
- Ashish, D. K. and Saini, P., Successive recycled coarse aggregate effect on mechanical behavior and microstructural characteristics of concrete, *Comput. Concr.*, 21(1), 39–46(2018). <https://doi.org/10.12989/CAC.2018.21.1.039>
- Bao, J., Li, S., Zhang, P., Ding, X., Xue, S., Cui, Y. and Zhao, T., Influence of the incorporation of recycled coarse aggregate on water absorption and chloride penetration into concrete, *Constr. Build. Mater.*, 239, 117845(2020). <https://doi.org/10.1016/j.conbuildmat.2019.117845>
- Brandt, A. M., Olek, J., & Marshall, I. H., Properties of fiber reinforced cement composites with cenospheres from coal ash. *Brittle Matrix Compos.*, 9, 245 (2009). <https://doi.org/10.1533/9781845697754.245>
- Bui, N. K., Satomi, T. and Takahashi, H., Improvement of mechanical properties of recycled aggregate concrete basing on a new combination method between recycled aggregate and natural aggregate, *Constr. Build. Mater.*, 148, 376–385(2017). <https://doi.org/10.1016/j.conbuildmat.2017.05.084>
- Carneiro, J. A., Lima, P. R. L., Leite, M. B. and Toledo F. R. D., Compressive stress–strain behavior of steel fiber reinforced-recycled aggregate concrete, *Cem. Concr. Compos.*, 46, 65–72(2014). <https://doi.org/10.1016/j.cemconcomp.2013.11.006>
- Cheng, Y., Shen, N., Yu, H., Feng, L., Yang, T. and Shen, J., Effect of Recycled Aggregate Content on Water Permeability and Pore Structure of Pervious Concrete Pavement, *Adv. Mater. Sci. Eng.*, 2022, 1–11(2022). <https://doi.org/10.1155/2022/4220122>
- Elanthikkal, S., Mohamed, H. H. and Alomair, N. A., Extraction of biosilica from date palm biomass ash and its application in photocatalysis, *Arabian J. Chem.*, 16(3), 104522(2023). <https://doi.org/10.1016/j.arabjc.2022.104522>
- Erdem, S., Dawson, A. R. and Thom, N. H., Microstructure-linked strength properties and impact response of conventional and recycled concrete reinforced with steel and synthetic macro fibers, *Constr. Build. Mater.*, 25(10), 4025–4036(2011). <https://doi.org/10.1016/j.conbuildmat.2011.04.037>
- Ganga, V. and Senthil, S. S., Influence of expansive cement on rheological, strength performance and morphological characteristics of self-compacting concrete, *Constr. Build. Mater.*, 368, 130407(2023). <https://doi.org/10.1016/j.conbuildmat.2023.130407>
- Gao, D. and Zhang, L., Flexural performance and evaluation method of steel fiber reinforced recycled coarse aggregate concrete, *Constr. Build. Mater.*, 159, 126–136(2018). <https://doi.org/10.1016/j.conbuildmat.2017.10.073>
- Gholampour, A. and Ozbakkaloglu, T., Fiber-reinforced concrete containing ultra high-strength micro steel fibers under active confinement, *Constr. Build. Mater.*, 187, 299–306(2018). <https://doi.org/10.1016/j.conbuildmat.2018.07.042>
- Guo, H., Shi, C., Guan, X., Zhu, J., Ding, Y., Ling, T. C., Zhang, H. and Wang, Y., Durability of recycled aggregate concrete A review, *Cem. Concr. Compos.*, 89, 251–259(2018). <https://doi.org/10.1016/j.cemconcomp.2018.03.008>
- Guo, Y. C., Zhang, J. H., Chen, G., Chen, G. M. and Xie, Z. H., Fracture behaviors of a new steel fiber reinforced recycled aggregate concrete with crumb rubber, *Constr. Build. Mater.*, 53, 32–39(2014). <https://doi.org/10.1016/j.conbuildmat.2013.11.075>
- Ibrahim, Y. E., Fawzy, K. and Farouk, M. A., Effect of steel fiber on the shear behavior of reinforced recycled aggregate concrete beams, *Struct. Concr.*, 22(3), 1861–1872(2021). <https://doi.org/10.1002/suco.202000494>
- Kannan, S., Arunachalam, K. and Brindha, D., Performance analysis of recycled aggregate concrete with chemical admixture, *Struct. Concr.*, 22(1), (2021). <https://doi.org/10.1002/suco.201900380>
- Karatas, M., Dener, M., Benli, A. and Mohabbi, M., High temperature effect on the mechanical behavior of steel fiber reinforced self-compacting concrete containing ground pumice powder, *Struct. Concr.*, 20(5), 1734–1749(2019). <https://doi.org/10.1002/suco.201900067>

- Kisku, N., Joshi, H., Ansari, M., Panda, S. K., Nayak, S. and Dutta, S. C., A critical review and assessment for usage of recycled aggregate as sustainable construction material, *Constr. Build. Mater.*, 131, 721–740(2017).
<https://doi.org/10.1016/j.conbuildmat.2016.11.029>
- Kou, S. C. and Poon, C. S., Properties of self-compacting concrete prepared with coarse and fine recycled concrete aggregates, *Cem. Concr. Compos.*, 31(9), 622–627 (2009).
<https://doi.org/10.1016/j.cemconcomp.2009>
- Liao, J., Li, F., Gong, J., Zhao, L., Tong, X. and Li, X., Durability of Recycled Concrete after Reinforcing the Aggregates with Permeable Crystalline Materials, *Adv. Civ. Eng.*, 2024(1), 1-14(2024).
<https://doi.org/10.1155/2024/9978563>
- Limbachiya, M., Meddah, M. S. and Ouchagour, Y., Use of recycled concrete aggregate in fly-ash concrete, *Constr. Build. Mater.*, 27(1), 439-449 (2012).
<https://doi.org/10.1016/j.conbuildmat.2011.07.023>
- Nanthini, M., Ganesan, R. and Jaganathan, V., Studies on Alkaline Activator, Manufacturing Methods and Mechanical Properties of Geopolymer Concrete A Review, Studies on Alkaline Activator, Manufacturing Method and Mechanical Properties of Geopolymer Concrete for Sustainable Environment A Review, *J. Environ. Nanotechnol.*, 13(3), 52–72(2024).
<https://doi.org/10.13074/jent.2024.09.242753>
- Poon, C. S., Kou, S. C. and Lam, L., Use of recycled aggregates in molded concrete bricks and blocks, *Constr. Build. Mater.*, 16(5), 281–289(2002).
[https://doi.org/10.1016/S0950-0618\(02\)00019-3](https://doi.org/10.1016/S0950-0618(02)00019-3)
- Ramkumar, K. B. and Kannan, R. P. R Impact of hybrid steel fibers on fresh and mechanical properties of Self-compacting concrete, *Case Stud. Constr. Mater.*, 17, e01274(2022).
<https://doi.org/10.1016/j.cscm.2022.e01274>
- Rao, C. M., Bhattacharyya, S. K. and Barai, S. V., Behaviour of recycled aggregate concrete under drop weight impact load, *Constr. Build. Mater.*, 25(1), 69–80(2011).
<https://doi.org/10.1016/j.conbuildmat.2010.06.055>
- Sampathkumar, V., Raja, K., Navaneethan, K. S., Lakshmi, N. J., Ambika, D., Manoj, S. and Kumar, K. S., Strength Characteristics of Bentonite Nano Clay Stabilized with Addition of Lime, Fly Ash, and Silica Fume for Soil Environmental Sustainability, *J. Environ. Nanotechnol.*, 13(2), 160–167(2024).
<https://doi.org/10.13074/jent.2024.06.242644>
- Scrivener, K. L. and Kirkpatrick, R. J., Innovation in use and research on cementitious material, *Cem. Concr. Res.*, 38(2), 128–136(2008).
<https://doi.org/10.1016/j.cemconres.2007.09.025>
- Senaratne, S., Gerace, D., Mirza, O., Tam, V. W. Y. and Kang, W. H., The costs and benefits of combining recycled aggregate with steel fibers as a sustainable, structural material, *J. Cleaner Prod.*, 112(4), 2318–2327(2016).
<https://doi.org/10.1016/j.jclepro.2015.10.041>
- Soroushian, P. and Lee, C. D., Distribution and orientation of fibers in steel fiber reinforced concrete. *Materials journal*, 87(5), 433-439 (1990).
<https://doi.org/10.14359/1803>
- Verma, S. K. and Ashish, D. K., Mechanical behavior of concrete comprising successively recycled concrete aggregates, *Adv. Concr. Constr.*, 5(4), 303–311(2017).
<https://doi.org/10.12989/ACC.2017.5.4.303>
- Wardeh, G., Ghorbel, E. and Gomart, H., Mix Design and Properties of Recycled Aggregate Concretes: Applicability of Eurocode 2, *Int. J. Concr. Struct. Mater.*, 9(1), 1–20(2015).
<https://doi.org/10.1007/s40069-014-0087-y>
- Xiao, J., Li, W., Fan, Y. and Huang, X., An overview of study on recycled aggregate concrete in China (1996–2011), *Constr. Build. Mater.*, 31, 364–383(2012).
<https://doi.org/10.1016/j.conbuildmat.2011.12.074>
- Yi, Y., Zhu, D., Guo, S., Zhang, Z. and Shi, C., A review on the deterioration and approaches to enhance the durability of concrete in the marine environment, *Cem. Concr. Compos.*, 113, 103695(2020).
<https://doi.org/10.1016/j.cemconcomp.2020.103695>